Proceedings of the
Annual Stability Conference
Structural Stability Research Council
San Antonio, Texas, March 19-22, 2024

The impact of analysis assumptions on buckling prediction in open-web steel joists

Kubilay Cicek[1], Thomas Sputo[2], Hannah B. Blum[3],

Abstract

Open-web steel joists are a common and highly efficient system for supporting floor or roof loads in long-span structures. They are often constructed using members with relatively high slenderness ratios, and as a result, may be susceptible to buckling instabilities in the webs and the compression chord. When the top chord is constructed using double angles, plates may be welded between the chord angles, and these "fillers" may serve the purpose of reducing the unbraced length of the individual angles. As part of a system reliability study on open-web steel joists, three different general failure modes were identified in common gravity-loaded joist designs: top chord buckling (lateral, torsional), bottom chord tension yielding, and first web member tension yielding. Furthermore, design by joist manufacturers is performed using results from a two-dimensional line-element model, which differs from the results of a three-dimensional shell-element model. Two open-web steel joist models are investigated, one with hot-rolled members and the other with cold-formed members. The details of each joist design are varied, including cross-section sizes of the members, to produce the desired failure modes through a line-element analysis assumption. Next, each joist design is created and analyzed with three-dimensional shell-element models that account for nonlinear material behavior. The resulting ultimate load, deflections, and failure mode are compared to the design predictions based on the line-element model. A discussion of the discrepancies in failure mode predictions due to the analysis assumptions are presented in addition to updated buckling failure estimations.

1. Introduction

Steel open-web joists provides an effective way to support floor and roof loads due to their lightweight and easy-to-implement nature. Steel joists can be manufactured using different cross sections and web geometries to most economically support required loading. Additionally, steel is well-known for its high elastic capacity and high post-yield ductility. This provides an extra margin of safety and flexibility in joist design. Steel joists are designed and fabricated in accordance with the

[1]Research Assistant, University of Wisconsin-Madison, <cicek@wisc.edu>
[2]Technical Director, Steel Deck Institute, <tsputo50@gmail.com>
[3]Assistant Professor and Alain H. Peyrot Fellow in Structural Engineering, University of Wisconsin-Madison, <hannah.blum@wisc.edu>

requirements of the SJI Standard (Steel Joist Institute, 2020), supplemented by the AISC Specification (American Institute of Steel Construction, 2016) or the AISI Standard (American Iron and Steel Institute, 2020) as required. Using this Standard, a large variety of both standard and non-standard steel open-web joists can be designed to support roof and floor loads.

For a system reliability study of steel joist systems, it was desired to study joist systems with several failure modes. The three failure modes of interest were bottom chord tension yielding, first web tension yielding, and top chord buckling. Two standard K-Series joists of 50-foot span were selected for the study, one joist with hot-rolled members and one joist with cold-formed members. SJI member companies designed the joists, and modifications were made to the joist designs to obtain the specific failure modes, such as by using smaller sections for specific members or removing the fillers to increase the slenderness.

Software used for 2D analysis by a joist manufacturer assumes a linear elastic material behavior, and accounts for global member instability by using effective length factors (K factors) contained in the SJI Standard (Steel Joist Institute, 2020). Web members are assumed to have pinned ends. Residual stresses, inelastic behavior, and out-of-straightness is accounted for in the compression strength equations in the SJI Standard (Steel Joist Institute, 2020) which are similar to those in the AISC Standard (American Institute of Steel Construction, 2016). These assumptions in the 2D model have an impact on the predicted limit states and nominal resistance of the joist. These assumptions are explained in section 7.

Advanced 3D finite element models (FEM) were created with shell elements in Abaqus. Instead of effective length factor assumptions, the actual connection lengths were directly modeled, and inelastic behavior and element buckling were included in the analyses. The resulting failure modes of the joists were compared with the anticipated failure modes from the design software. Additionally, the nominal resistance and maximum deflections are also compared against the joist manufacturer's in-house beam element software results. The comparisons show that there are differences between the limit states, ultimate strength, and deflection values. The limit state of top chord compression buckling showed the greatest deviation between the manufacturer's software design predictions and the 3D shell FE models. A discussion on the design assumptions and impact on the joist failure modes are presented.

2. Selected Joist Designs

The joist designs considered in this study were provided by the SJI member manufacturers. Generic layouts of these joists are taken from manufacturer design sheets and given in Figure 1 for Joist I (hot-rolled steel members) and Figure 2 for Joist II (cold-formed steel members). Both joists are 30 inches deep with a 50 foot span and have similar design loads. Fillers are used in both joists and placed at the midpoint between panel points where top chord compression forces are highest. According to the manufacturer design sheets, Joist I has fillers in the middle four panels, and Joist II has fillers in the middle six panels and additionally one filler each in the end panels. The initial designs of these joists were modified to obtain the selected limit states under the maximum loading conditions. Depending on the selected limit state, e.g., bottom chord tension yielding, the bottom chord section size was decreased. The maximum design loads were also updated according to the updated section dimensions and these updated maximum loads were used in the FE models. Under

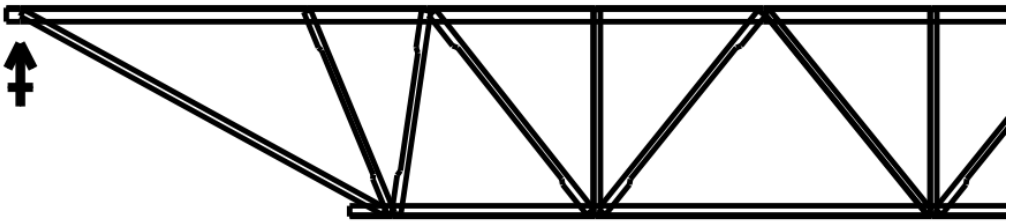

Figure 1: Joist with HRS sections and crimped angle webs (Joist I)

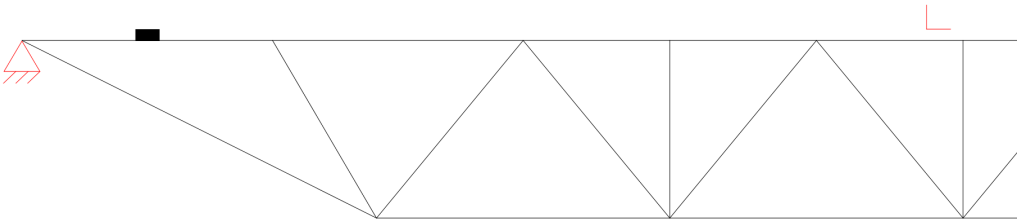

Figure 2: Joist with CFS angle and channel sections (Joist II)

all these assumptions, six different joists models (two different joists models with three different failure modes) are designed and used in this study. Detailed 3D shell element FE models were generated to determine the failure modes and to compare with the design software predictions.

Joist I (HRS) has single angle sections for the web elements, double angles for the chords, and round rod sections for the first web on both ends of the joist. Web angles are crimped at both ends starting from 6 inches from the end of the member to fit between the chord angles. Joist II (CFS) uses channel sections for all the webs (including the end web) and angle sections for chord members. These sections types can be seen in Figure 3.

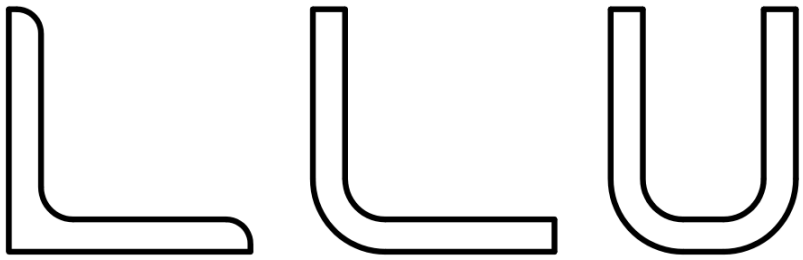

Figure 3: Left: HRS angle, Middle: CFS Angle, Right: CFS Channel sections

3. Joist Design Assumptions

The joists are designed using linear elastic proprietary software by the manufacturer. All members are modeled using 2D beam elements. The software selects the individual members based on built-in algorithms which incorporate the requirements of the SJI Standard (Steel Joist Institute, 2020). Safety factors (ASD) or Resistance factors (LRFD) are applied on a member by member basis to determine the design load. Because of consistency in the safety factors, the ultimate resistance of the joist is 1.67 times the ASD design load. Welds are designed using the SJI weld design method. The SJI Standard references the AISC 360 Standard (American Institute of Steel Construction,

2016) and the AISI S100 Standard (American Iron and Steel Institute, 2020) respectively for hot-rolled and cold-formed sections where the SJI Standard is silent.

Since the proprietary 2D beam element software performs an elastic analysis, the non-linear behavior of the members is not considered in the design. Because a joist is an indeterminate structure, the consideration of inelastic behavior can increase the ultimate resistance of the joist compared to an elastic analysis. However, as it can be shown in experimental studies (Sadowski et al., 2015 and Young and Rasmussen, 1999) or in material models (Yun and Gardner, 2017 and Gardner and Yun, 2018), HRS and CFS sections have different nonlinear behaviors which affect the ultimate resistance when inelastic analysis is performed.

In accordance with the SJI Standard (Steel Joist Institute, 2020) the ends of the web members are considered to be pins without rotational restraint. However, actual webs on joists are welded to chord members which provides an amount of rotational resistance. The weld length and web section dimensions affect the rotational stiffness, and therefore, the end behavior of webs at every panel points will differ. Considering the actual rotational restraint at the web member ends potentially reduces the effective unbraced length of compression members, and reduces the deflection of the joist when compared against the pin-ended web model.

The proprietary software used by SJI manufacturers incorporates the effective length factors (K-factors) for design of compression members. These effective length factors are stipulated in Table 4.3-1 of the SJI Standard (Steel Joist Institute, 2020).

MAXIMUM AND EFFECTIVE SLENDERNESS RATIOS[1]					
Description			$k\ell/r_x$	$k\ell/r_y$	$k\ell/r_z$	$k\ell_s/r_z$
I.	TOP CHORD INTERIOR PANELS					
	A.	The slenderness ratios, $1.0\ell/r$ and $1.0\ell_s/r$, of members as a whole or any component part shall not exceed 90.				
	B.	The effective slenderness ratio for joists, $k\ell/r$, to determine F_{cr} where k is:				
		1. Two shapes with fillers or ties	0.75	0.94	---	1.0
		2. Two shapes without fillers or ties	---	---	0.75	---
		3. Single component members	0.75	0.94	---	---
	C.	For bending, the effective slenderness ratio, $k\ell/r$, to determine F'_e where k is:	0.75	---	---	---

Figure 4: Effective length factors (K-factors) for design of compression members, copied from Table 4.3-1 in the SJI Standard (Steel Joist Institute, 2020)

In typical joist designs, fillers are included between the top chord angles where the compression forces are highest to decrease the unbraced buckling length of the individual angle, and increase the compressive strength of the chord. In the provided joist designs for the top chord buckling limit state, the cross-section sizes of an individual top chord angle is decreased or fillers are removed to increase the unbraced length and drive a limit state of torsional buckling of an individual angle. Without the fillers, the unbraced buckling length equals to the distance between panel points multiplied by the SJI mandated effective length factor. As a result, proprietary software will predict a lower compression strength for the top chords. Table 4.3-1 (Steel Joist Institute, 2020) neglects the contribution of attached steel deck in restraining x- and z- axis buckling which is substantial in the erected structure.

A serviceability limit state of $L/360$ deflection at mid-span is considered as recommended by the SJI Standard (Steel Joist Institute, 2020). For the joists under consideration, this equates to a maximum serviceability limit of 1.67 inches for both joists under design loads. The design loads are limited by the serviceability limit for each joist design in SJI in-house software. These design loads and deflections at design loads were provided so that results from the 3D shell element model could be validated by comparing mid-span deflections at the applied design loads. The design predictions from the SJI in-house software also provides anticipated ultimate loads for each of the six joists (three different failure modes for both HRS and CFS joists). From this information, ultimate loads from the 3D shell element model can be compared to the predicted ultimate loads from the SJI software.

4. Finite Element Models

Finite element models of the provided joists are generated in Abaqus software (Abaqus, 2016). Joists are primarily manufactured by using open sections such as angles and channel sections, and solid sections such as round rod. All sections are modeled with S4R shell elements except for the round rod and the filler elements between the chord angles which are modeled with C3D8R solid elements.

Welds between open section shell elements are modeled as tie connections using edge lines of shell elements for weld lines (Figure 5). However, the weld connections between solid elements (rods and fillers) and chord angles are represented by surface to surface tie connections. Double bevel welds are used for the welded connection of rods and fillers to the chord angles (Figure 6). These double bevel welds are modeled with a separate weld element and a welding material, which was modeled with 517 MPa (75 ksi) yield strength material. Therefore, a surface to surface tie connection is preferred for the connection between weld elements and joist elements.

Weld lengths were specified in the design drawings. Where the webs are connected to the chord angles, only the top side of the top chord-web connection and the bottom side of the bottom chord-web connection is welded to reflect realistic welds considering the welder position. This is reflected in the FE models as shown in Figure 6.

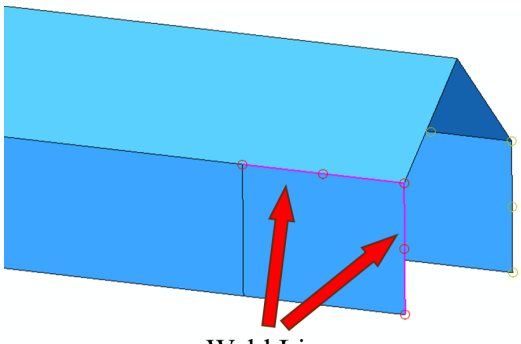

Figure 5: Weld line tie connections for open section welds shown on a crimped angle web

The crimped angle webs are also represented in the finite element models. Transition from the uncrimped angle to the crimped portion starts from 15 cm (6 inches) from the ends (Figure 7). Including the crimping in the FE models affects the webs under compression. It also provides a

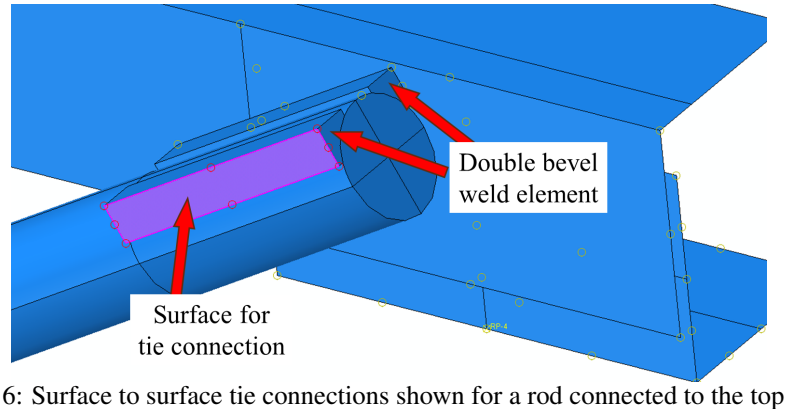

Figure 6: Surface to surface tie connections shown for a rod connected to the top chord

better approach to obtain the true influence of welded web connections in joists under loading.

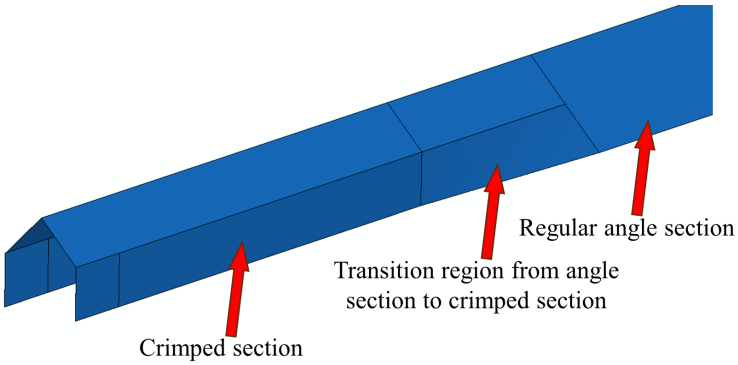

Figure 7: HRS angle web crimped at 6 inches at the ends

4.1 Material Models

As the results may be sensitive to yielding of the members and post-yielding behavior, detailed material models were included in the FE models for both hot-rolled steel and cold-formed steel. Sadowski et al. (2015) and Young et al. (1999) show that the post-yield nonlinear behaviors of HRS and CFS show significant differences. The HRS section material model used in this study is taken from the study of Yun et al. (2017) and the CFS section material model is taken from the study of Gardner et al. (2018). In both of these studies, dozens of test data from various published experimental studies were collected and analyzed to predict representative material models. A representative stress-strain curve can be generated with only a known yield stress.

The stress-strain curves used in this study based on the nominal yield stress are shown in Figure 8. The yield stress of both materials are 345 MPa (50 ksi) and the elastic modulus is 200 GPa (29,000 ksi) for HRS (American Institute of Steel Construction, 2016) and 203.4 GPa (29,500 ksi) for CFS (American Iron and Steel Institute, 2020). The stress-strain curves are converted to true stress and true strain for implementation into Abaqus.

4.2 End and Lateral Supports

The joist system is modeled as simply supported with a pin support at one end and a roller support at the other end. In physical joists, angle section seats are welded at the end of the both top chords

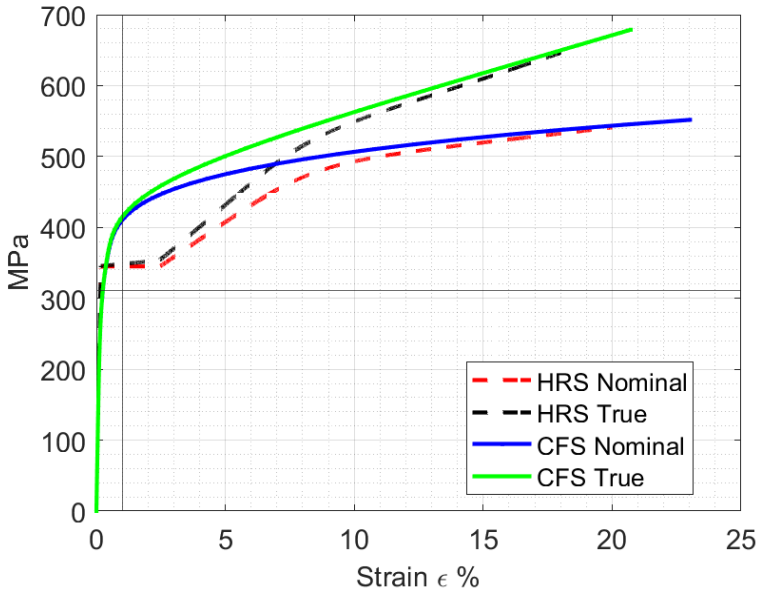

Figure 8: Material models for HRS and CFS sections

of the joists, and the welded seats are placed on girders or other supports. The angle seats are also modeled with shell elements as shown in Figure 9. The pin and roller supports are applied to the seat angle corner at the midpoint.

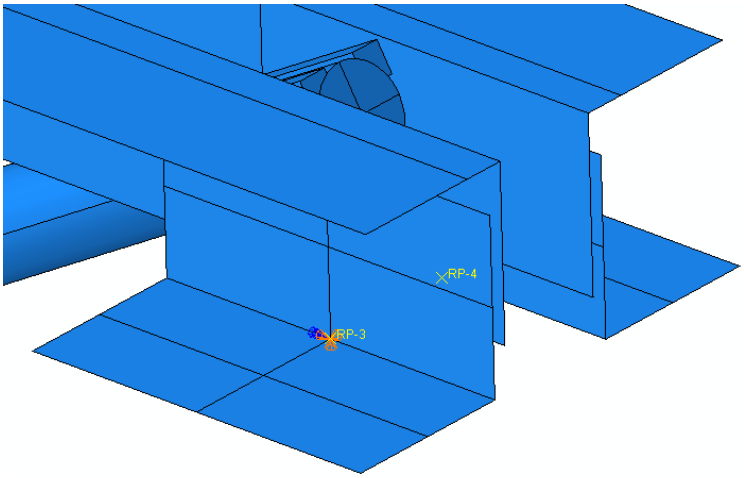

Figure 9: Seats at joist ends

The out of plane movement of joists was also restrained by considering the actual positions of lateral supports in the physical joists. Out of plane constraints are included in shell element models and are defined at every panel point in the bottom chord (Figure 10) and at every 12 inches on top chords (Figure 11).

4.3 Loads

Loads are applied on the top side of the top chord angle sections near the heel as a uniformly distributed load. The load position is shown in Figure 12. This positioning of loads is preferred to

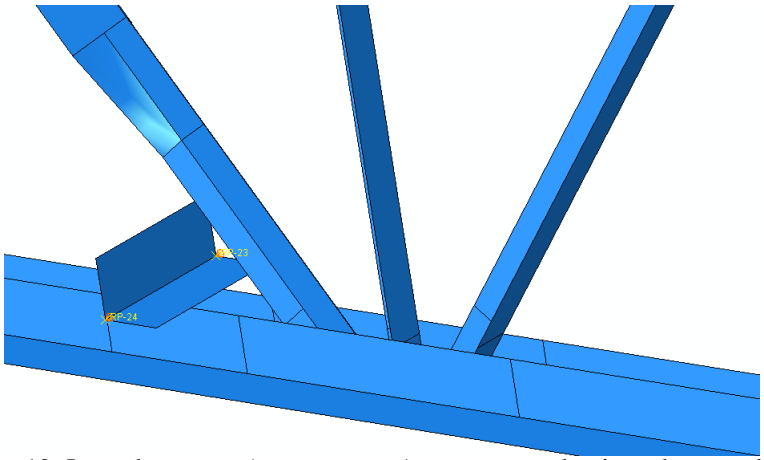

Figure 10: Lateral supports (orange arrows) at every panel point at bottom chords

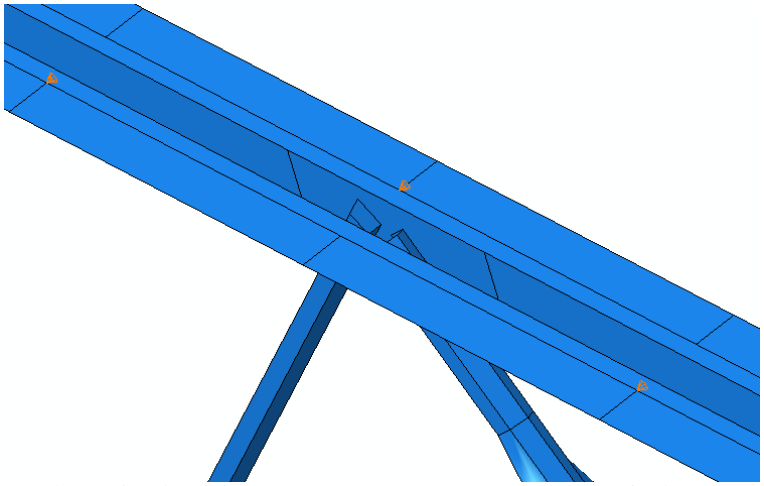

Figure 11: Alternating lateral supports (orange arrows) at every 12 inches on top chords

avoid additional torsional forces that can result from applying loads to the tip of angle sections.

4.4 Analysis

Two types of analyses were run for all models, second order inelastic and Riks. Second order inelastic analyses were used to (1) validate the models by comparing mid-span deflections of the joists with applied design loads to the deflections predicted by SJI at design loads (recall, design loads were limited by serviceability), and (2) compare joist output and failure modes at the SJI predicted ultimate loads. The Riks analysis was used to determine the ultimate capacity, failure mode, and to the post-peak behavior of the joist system. Second order effects and nonlinear material behaviors were included in both analyses. In the second order inelastic analyses, the load was applied in increments of 10% of the design load. In the Riks analysis, the load factor increment was limited to a maximum of 0.1 of the predicted ultimate load.

5. Results

This section includes the finite element model results for both joists including failure modes, ultimate loads, stresses, and deflections. First, the models were validated by comparing deflections

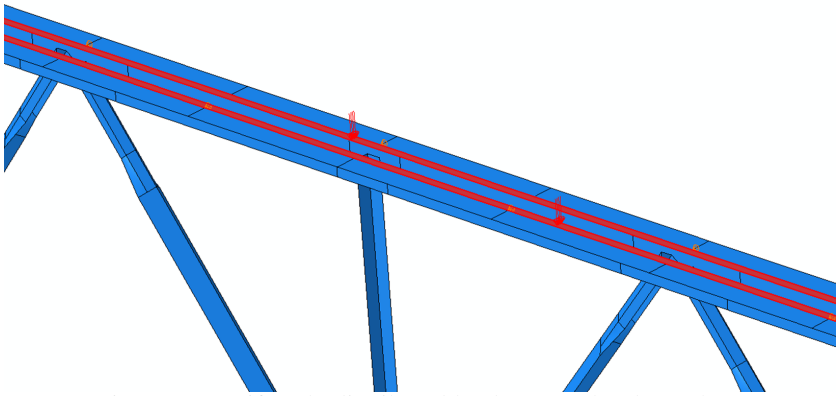

Figure 12: Uniformly distributed load on top chord members

Table 1: Vertical deflection at midspan comparison between manufacturer model predictions and FE shell element models results under design loads

	Joist I			**Joist II**		
Failure Mode Model	SJI-model (in)	Shell Elem (in)	Diff (%)	SJI-model (in)	Shell elem (in)	Diff (%)
Bot. Chord	1.67	1.685	0.9	1.6	1.636	2.2
First Web	1.6	1.642	2.55	1.6	1.6	0
Top Chord	1.6	1.614	0.9	1.6	1.63	1.8

at design loads. Next, predicted ultimate loads were applied and second order inelastic analyses were run. The results were used to compare behavior and failure modes between the 3D shell element models and SJI failure modes at SJI predicted ultimate loads. Lastly, Riks analyses were run to determine ultimate loads and failure modes of the 3D shell element models. These results were used to compare the failure modes of each joist design to the failure mode predictions based on proprietary manufacturer software which uses 2D beam elements and the other assumptions provided in Section 3.

5.1 Model Validation

To validate the FE modeling method, design loads were applied to the joists and second order analyses were run. Bottom chord mid-span deflections were recorded and compared to manufacturer software-predicted deflections, and are presented in Table 1. The small percent difference indicated close behavior predictions at design loads.

5.2 Bottom Chord Yielding

At predicted ultimate loads, the bottom chords have the highest tensile stresses and the mid-span of the bottom chord is close to reaching yield stress (around 310 MPa or 45 ksi) in both joist designs. However, the manufacturer's in-house software showed that the chord angle sections reach yield at predicted ultimate loads.

The Riks analyses results indicated a bottom chord yielding failure. Figure 13 shows the applied load factor, where 1 is the predicted ultimate loads, vs. bottom chord midspan vertical deflection

results of both joists. The bottom chord member sections are fully yielded and nearly reached ultimate material limit at mid-span (Figure 14). Large deflections occur due to material yielding of the bottom chord around midspan.

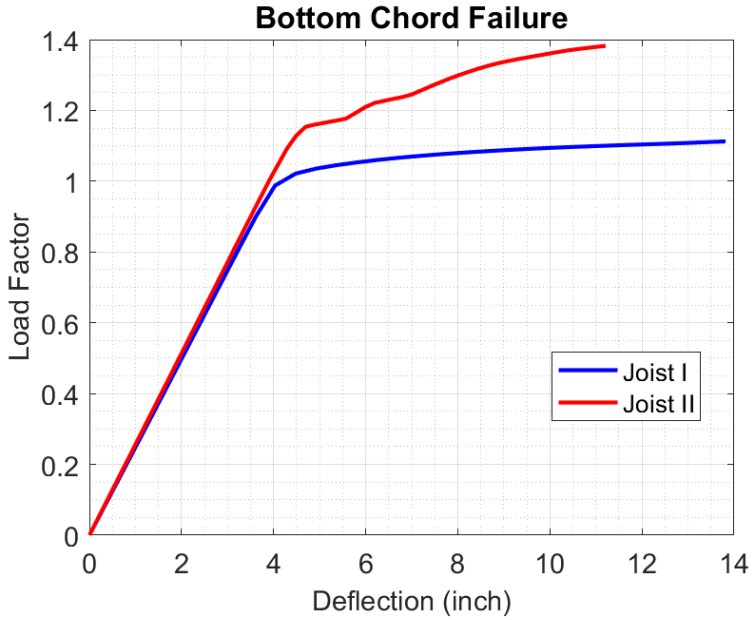

Figure 13: Load factor (1 = predicted ultimate loads) vs. midspan bottom chord deflection of joists with Riks analysis results for bottom chord yielding failure mode

5.3 First Web Yielding

At predicted ultimate loads, the first webs are designed fail due to tensile yielding. The results of the 3D shell FE model at ultimate loads resulted in web stresses of 280 MPa (41 ksi) for Joist I and 270 MPa (39 ksi) for Joist II in the mid-length of the first web. However, the maximum web stresses occurred at the connections and are close to yield stress (between 380 MPa (48 ksi) and 390 MPa (49 ksi)) due to the additional moments caused by welded connections between the webs and the chords.

The load factor vs. bottom chord mid-span deflection for the Riks analysis is shown in Figure 16. For Joist II, the highest stresses are on the first web and failure is due to yielding of the first web channel section. Bottom chord angles are also yielding at the midspan region. However, the results for Joist I show that the bottom chord angles reach ultimate stresses before the first web, and hence failure is due to yielding in the bottom chord. This can be explained with the difference in the first web section between Joist I and Joist II.

Both ends of the first web members are subjected to in-plane rotational forces due to the deflected shape of the joist and welded connections. These high stress regions on first web ends can be seen in both joists as shown in Figures 16 and 17. A rod section is used for the first webs in Joist I and has a higher moment of inertia than an open channel section (Joist II). This explains why the failure mode for Joist I was bottom chord yielding rather than first web yielding. This also indicates that considering the web end connections as fully pinned, which is the method for SJI design calculations, can result in incorrect capacity and failure mode predictions.

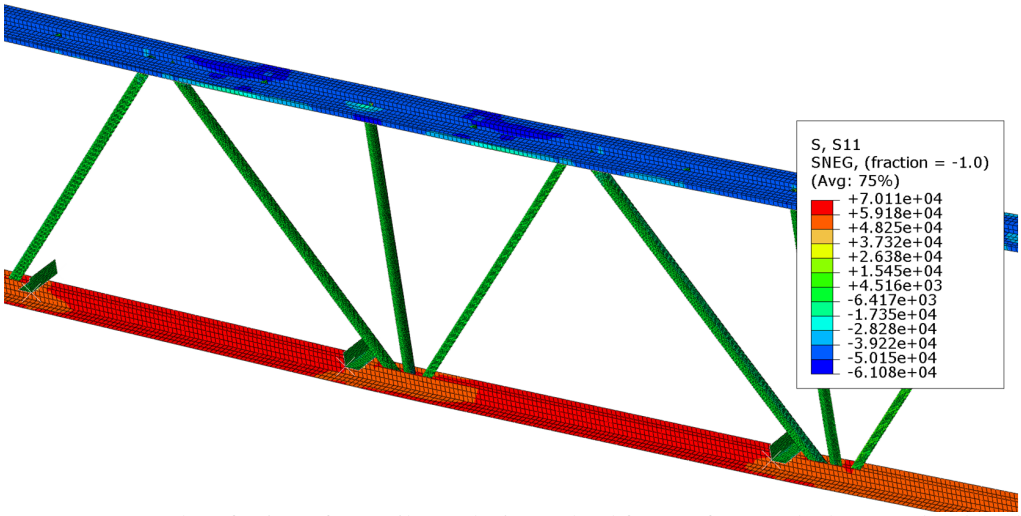

Figure 14: Stress contour plot of Joist II from Riks analysis at a load factor of 1.38. The bottom chord angles are fully yielded at the joist midspan. Units: ksi

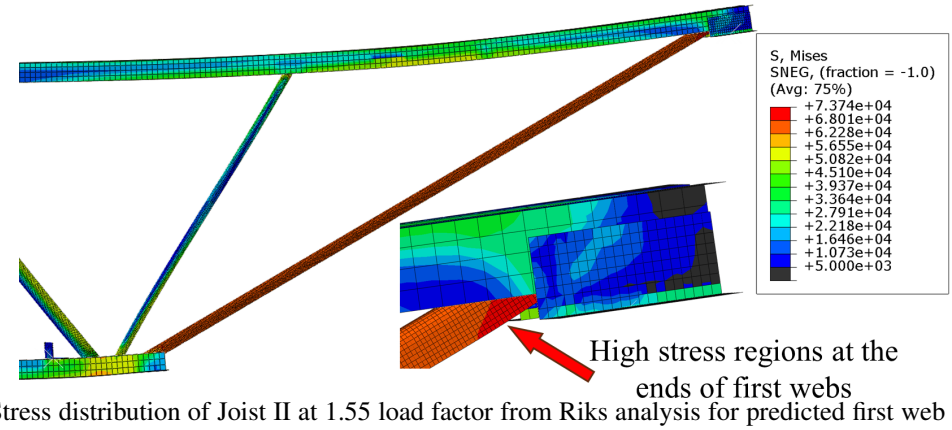

Figure 16: Stress distribution of Joist II at 1.55 load factor from Riks analysis for predicted first web yielding failure mode. The first web is fully yielded and has reached ultimate stress of the material. Units: ksi

5.4 Top Chord Buckling

Top chord buckling results are the most conflicted results between the manufacturer's software predictions and FE model results. At predicted ultimate loads, there is no buckling nor yielding in any sections and the highest stresses (around 300MPa or 43 ksi) are in the bottom chord angles.

Top chord buckling failure does not occur in the Riks analysis for either joist. The bottom chord fully yields and the load cannot increase sufficiently to result in top chord buckling after bottom chord yielding occurs. The load ratio vs. midspan bottom chord vertical deflection for both joists are shown in Figure 18.

The reason behind this difference in 3D shell FE vs. predicted behavior is that manufacturer's proprietary design software assumes web members are pinned without any rotational restraint. However, the web weld length and connectivity to the chord provides some rotational restraint. Further discussions regarding the effective length assumptions are provided in Section 7.

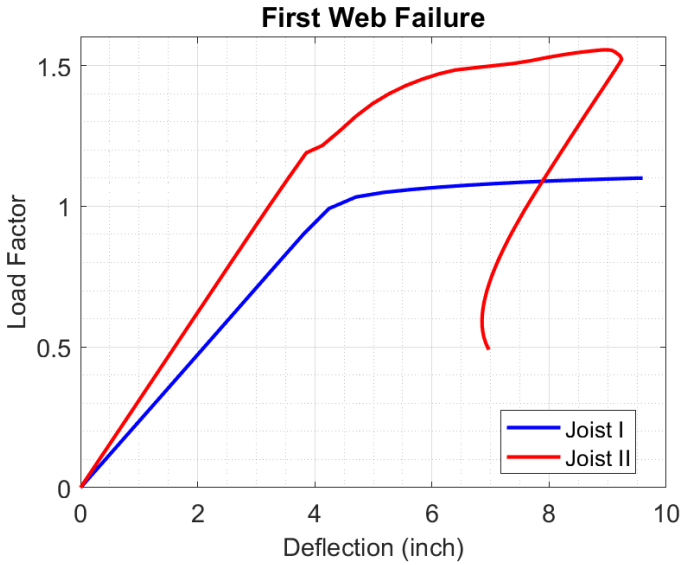

Figure 15: Load factor (1 = predicted ultimate loads) vs. midspan bottom chord vertical deflection of joists with Riks analysis results for predicted first web yielding failure mode

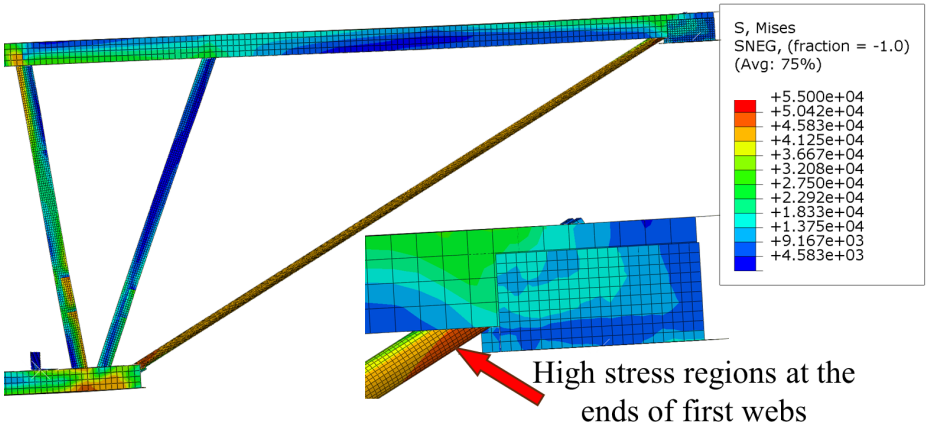

Figure 17: Stress distribution of Joist I at 1.1 load factor from Riks analysis for predicted first web yielding failure mode. The first web is partially yielded but has not reached ultimate stress of the material. Units: ksi

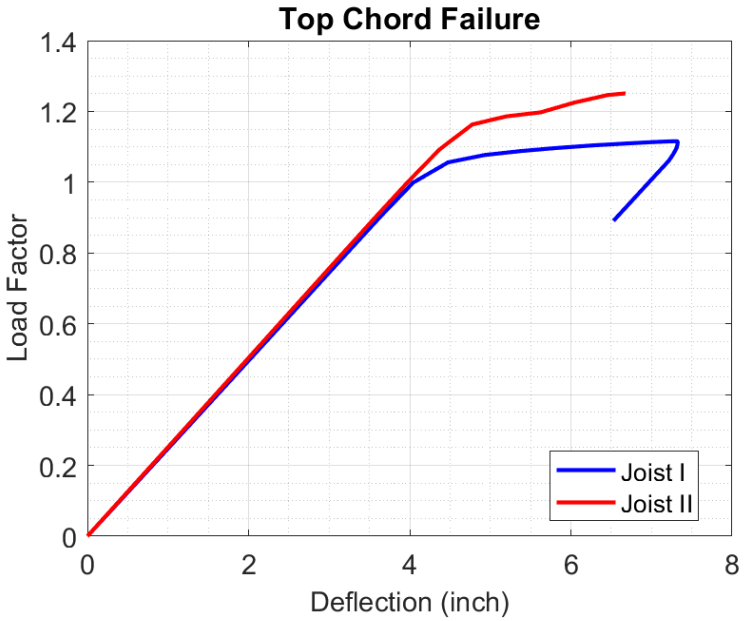

Figure 18: Load factor (1 = predicted ultimate loads) vs. midspan bottom chord vertical deflection of joists with Riks analysis results for predicted top chord buckling failure mode

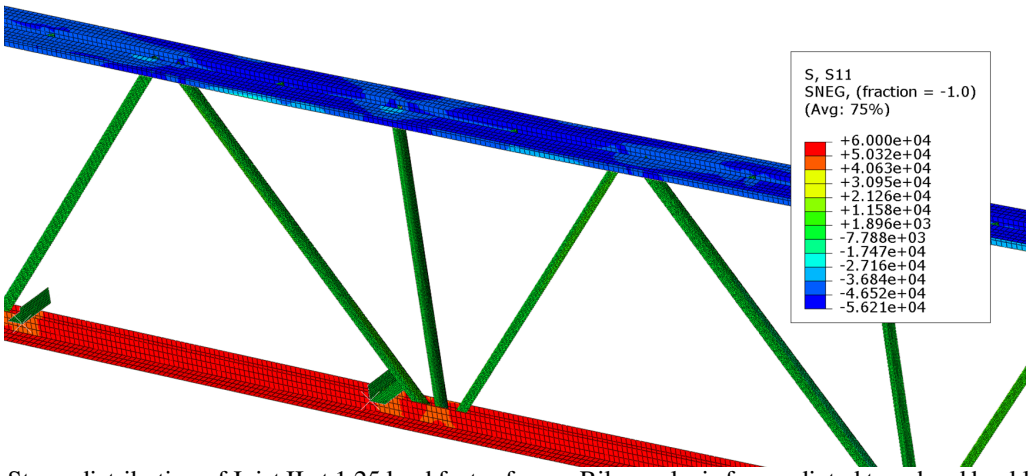

Figure 19: Stress distribution of Joist II at 1.25 load factor from a Riks analysis for predicted top chord buckling failure mode. Yielding on both top and bottom chords is visible.

6. Parametric study

It was desired to determine if top chord buckling could be achieved with Joist I and Joist II in the 3D shell FE model. Several parameters were changed to determine if those modifications could influence top chord buckling. Investigated parameters include removing fillers between the back-to-back chord members, adding in initial imperfections, and moving the positions of top chord lateral restraints. Each of these parameters was investigated separately where all other values remained at their nominal values.

6.1 Fillers between chords

In joist manufacturing, fillers are welded to both chord angles in top and bottom chords. Using fillers decreases the slenderness of the single angle by creating a composite section with the two back-to-back single angles, and therefore increases the top chord buckling resistance under compression forces. Fillers affect the buckling mode of the connected angles and the effect of fillers has been previously studied (Sippel, Ziemian, and Blum, 2022). The fillers were removed completely from both joists and the Riks analyses were run.

Removing the fillers out of the models did not result in top chord buckling. However, it increased the compression stress values slightly in mid-span of top chord elements. It also slightly reduced the maximum load factor of both joists.

6.2 Initial Imperfections

Member initial imperfections have a crucial effect on buckling load and buckling location. With the use of perfect geometry in the FE model software, it may be difficult to promote a buckling failure. It is recommended to use $L/1000$ initial imperfection in literature (Galambos, 1998).

Literature shows that the first buckling mode of angle sections also depends on the unbraced length of the member as shown in Dinis et al. (2010). This study shows that angle sections with unbraced length between 30 cm (12 in) to 80 cm (31.5 in) have pure torsional buckling, and angles with higher than 80 cm of unbraced lengths can have either flexural-torsional buckling or pure flexural buckling. Pure torsional buckling mode is used in this study since the distance between panel points can be considered as the maximum unbraced length, which is 60 cm (24 in), and the distance between fillers and panel points can be considered as the shortest unbraced length, which is 30 cm (12 in). And at this interval, the dominant buckling mode is pure torsional buckling.

Eigenvalue analyses are completed in Abaqus for top chord angles with 12 and 24 inches of unbraced lengths. The first mode of top chord angle sections in this study are founded to be torsional buckling mode (Figure 20) which is in compliance with the previous study results. $L/1000$ initial imperfections are implemented on top chord angles on the joist FE models in Abaqus and Riks analyses are completed with the initial imperfections.

With initial imperfections of $L/1000$, top chord buckling did not occur. Even when the initial imperfections were increased to $L/500$, the top chord buckling still did not occur.

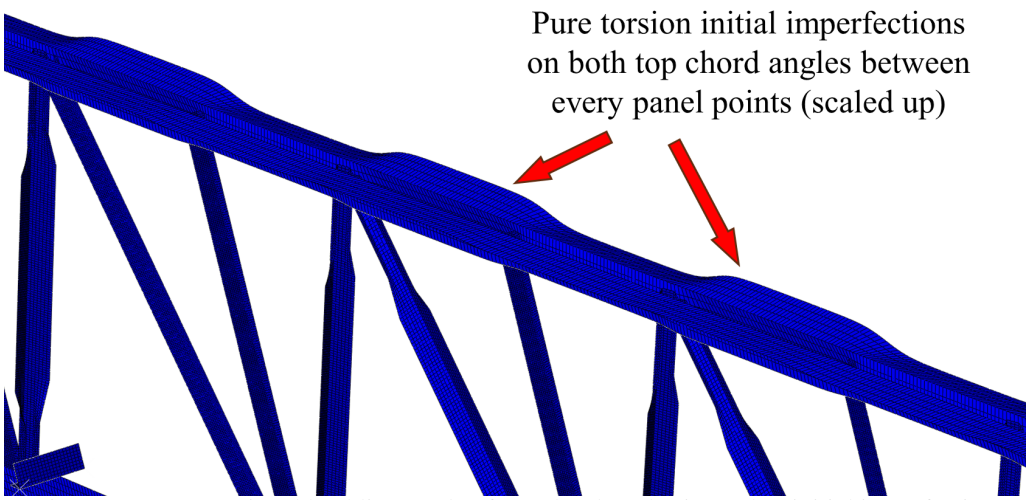

Figure 20: Pure torsional buckling mode of top chord angles is used as initial imperfection

6.3 Top Chord Lateral Restraints

Another assumption was the distance of lateral supports on top chord members. These are selected as 12 inches in FE models to represent the spacing of attachment of the steel deck to the joist chord. Lateral supports decrease the unbraced length leading to decreased slenderness ratio of the top chord segments. Increasing this distance might lead to out-of-plane movement and therefore, can trigger member buckling in top chord angles. To investigate the effect of lateral support spacing, the original models were updated to increase the lateral support spacing to 24, 36 and 48 inches. The results were compared to the original 12 inches spacing model. Buckling did not occur in any of the models.

6.4 Various Yield Stresses Among Joist elements

Another method to obtain the top chord buckling is to run the analyses with different yield stress values in different elements. Decreased yield stress value in top chord material can cause an early buckling response. Members in manufactured joists may have a variety of yield stresses due to the different sources of materials and providers. Therefore, the results of four different analyses were compared, each with the following material assumptions:

1. All members have nominal yield strength
2. Top chord members have nominal yield strength while all other members have increased yield strength (518 MPa [75 ksi])
3. Top chord members have decreased yield strength (310 MPa [45 ksi]), while all other members have nominal yield strength
4. Top chord members have decreased yield strength (310 MPa [45 ksi]), while all other members have increased yield strength (518 MPa [75 ksi])

The first condition is the standard design assumption that all the materials have the same yield strength of 345 MPa (50 ksi), which was discussed in Section 3. The second condition tests if the

buckling could occurs with the nominal yield stress of 345 MPa (50 ksi) for the top chord angles and an increased yield stress for the remainder of the members. The yield stress was increased up to 518 MPa (75 ksi), however this did not result in top chord buckling for Joist I. For Joist II, however, top chord buckling did occur when the other members yield stress was increased to 428 MPa (62 ksi).

The third and the forth conditions, where the top chord material yield strength was decreased (310 MPa [45 ksi]), both resulted in top chord buckling. An example of this result for condition four is shown in Figure 21. As the yield stress value for the top chord material is decreased (310 MPa [45 ksi]), the applied load factor at buckling failure is decreased. The difference between condition three (remaining members have nominal yield strength) and condition four (remaining members have increased (518 MPa [75 ksi]) yield strength) is the maximum load factor at which top chord buckling occurs. The main enabler of top chord buckling is the decreased yield strength in the top chord members, however, a yield strength of 310 MPa (45 ksi) in the top chords while the rest of the joist members have a yield strength of 345 MPa (50 ksi) may not be realistic.

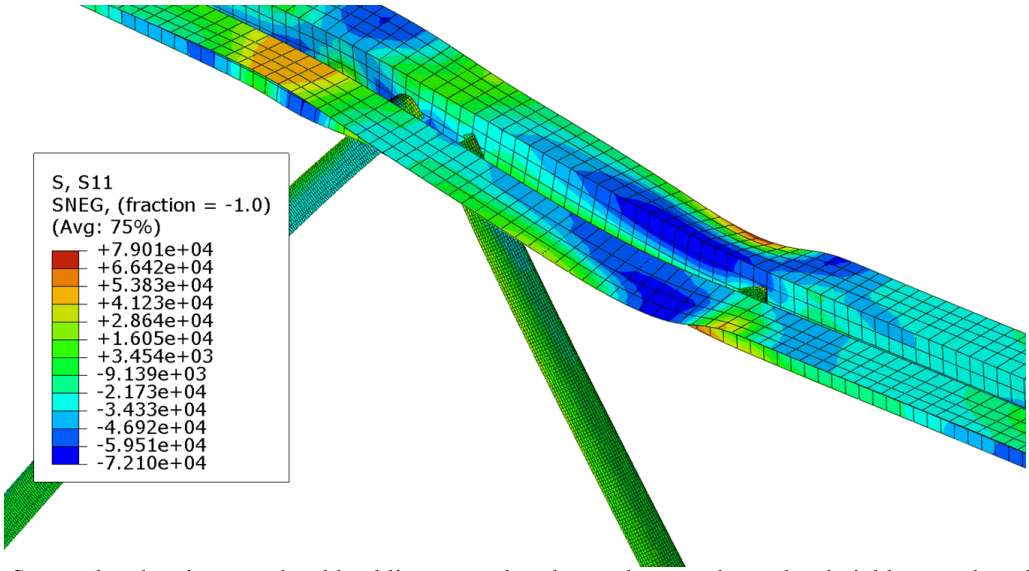

Figure 21: Stress plot showing top chord buckling occurring due to decreased top chord yield strength and increased yield strength for the remaining members

6.5 Combined Imperfections and Increased Lateral Restraint Spacing

To force top chord buckling, a model with increased spacing between lateral supports and initial imperfections was created for both Joist I and II. The lateral support spacing was increased to 24 inches and included $L/500$ magnitude imperfections. The combination of increased unbraced length and initial imperfection resulted in top chord buckling in a panel point without fillers as shown in Figure 22. Note that buckling did not occur with the standard $L/1000$ imperfection magnitude.

7. Discussion on effective length assumptions

Table 4.3-1 of the SJI Standard (Steel Joist Institute, 2020) provides effective length factors, K, for design of compression elements of the joist. For the top compression chord of the joist, for two

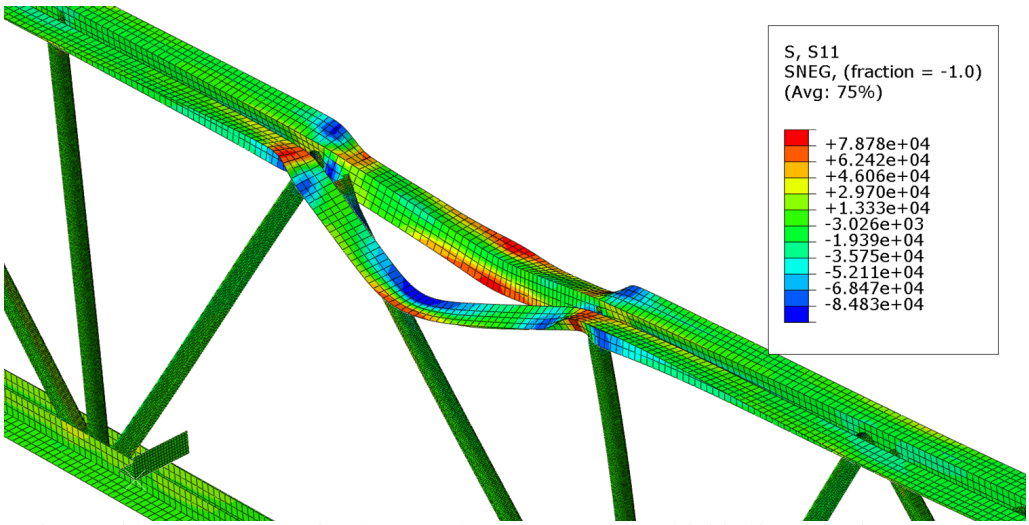

Figure 22: Joist II with 24 inches spacing between lateral supports, and initial imperfections resulted in top chord buckling where there were no fillers

angles with fillers or ties, the effective length factors provided in Table 2 are required. A review of the buckled shapes from the 3D shell element models, compared to the buckling strength from those models, leads to some observations about effective length factors for design.

Table 2: Effective length factor and slenderness ratio for three axes of buckling

	K	Slenderness Ratio	
For buckling vertically (x-axis)	0.75	KL/r_x	L = length center to center of panel points
For buckling out-of-plane of the joist (y-axis)	0.94	KL/r_y	L = 36 inches
For axis of least radius of gyration (z-axis)	1.0	KL_s/r_z	L_s = spacing between panel point and filler

Y-axis buckling is out-of-plane bucking of the built-up section of the two angles. This case did not control any of the joists in this study, and by rational observation it should not. However, if the steel deck is attached using the maximum fastener spacing permitted by the applicable SDI Standard (Steel Deck Institute, 2022) of 12 inches, the unbraced length L for this case should be the fastener spacing and, in that instance, it would never control. For the case where the top chord supports standing seam roofing or another panel that should not be relied upon for lateral bracing, the actual spacing of bridging would be used. The stipulated value of $K = 0.94$ is probably conservative for this mode because the angles are singly symmetric for this buckling mode, and the effective length factor for a compression member with fixed-fixed ends (0.6 to 0.7) would be more rational.

X-axis buckling is flexural buckling of the built-up section of the two angles and never controlled for any joists in this study. The stipulated unbraced length as being between panel points is reasonable and the stipulated effective length factor of 0.75 is also rational.

For Z-axis buckling, this study showed that the effective length factor of 1.0 is quite conservative. From both observations of the buckled shape and calculations considering flexural-torsional buckling, the effective length factor for design should be in the range of 0.6 to 0.7, depending on the rigidity of the welds at the fillers and panel points. This buckling limit state controlled in many instances, and as such, the design effective length factor warrants additional study.

8. Conclusions

Open-web steel joists are a common system to support roof and floor loads. Joists can be manufactured with a variety of cross-sections to provide the most economical design and can therefore be subjected to several failure modes. In this study, two joist designs, one hot-rolled steel and one cold-formed steel, were modified to result in three failure modes: bottom chord yielding, first web tension yielding, and top chord buckling. Failure mode and ultimate load predictions were determined by manufacturer's in-house software. The software uses 2D beam elements and assumes linear material behavior, pin-ended web connections, and specific effective length K factors. Detailed 3D finite element models were created of the joists using shell elements, non-linear material properties, and direct modeling of the welded web connections. The ultimate loads and failure modes resulting from the detailed finite element analysis were compared to the predictions produced by the manufacturer's in-house software.

Results show that the bottom chord yielding failure occurs in both joists as predicted, but at a slightly higher load level. The first web yielding failure was affected by the web-to-chord welded connections, which did not behave like pinned connections as predicted by the design method. Joist II (CFS) experienced yielding in both the end web and bottom chord at failure, while Joist I (HRS) failed due to bottom chord yielding. High stress concentrations occurred at the web ends. Top chord buckling failure did not occur for either joist and those models instead failed due to bottom chord yielding. The difference between actual and predicted behavior is a result of the effective length assumptions used in design. To assess when top chord buckling could occur, a parametric study was conducted where imperfections, fillers, lateral restraint locations, and yield strength were varied. It was found that top chord buckling could occur if the top chord yield strength is reduced relative to the other joist elements, or with increased spacing between lateral supports combined with larger than typical initial imperfections.

References

Abaqus (2016). *version 6.16*. Dassault Systèmes Simulia Corp.

American Institute of Steel Construction (2016). *Specification for structural steel buildings ANSI/AISC 360-16*. Chicago, IL, U.S.A.

American Iron and Steel Institute (2020). *S100-16 (R2020): North American Specification for the Design of Cold-formed Steel Structural Members*. Washington, DC, U.S.A.

Dinis, Pedro B, Dinar Camotim, and Nuno Silvestre (2010). "On the local and global buckling behaviour of angle, T-section and cruciform thin-walled members". In: *Thin-Walled Structures* 48.10-11, pp. 786–797.

Galambos, Theodore V (1998). *Guide to stability design criteria for metal structures*. John Wiley & Sons.

Gardner, Leroy and Xiang Yun (2018). "Description of stress-strain curves for cold-formed steels". In: *Construction and Building Materials* 189, pp. 527–538.

Sadowski, Adam J et al. (2015). "Statistical analysis of the material properties of selected structural carbon steels". In: *Structural Safety* 53, pp. 26–35.

Sippel, Edward J, Ronald D Ziemian, and Hannah B Blum (2022). "Influence of torsional stiffness in double-angle open-web joist and joist girder chords". In: *Journal of Constructional Steel Research* 199, p. 107595.

Steel Deck Institute (2022). *ANSI/SDI SD-2022, Standard for Steel Deck*.

Steel Joist Institute (2020). *ANSI/SJI 100 – 2020, Standard Specification for K-Series, LH-Series, and DLH-Series Open Web Steel Joists, and for Joist Girders*. Florence, SC, U.S.A.

Young, Ben and Kim JR Rasmussen (1999). "Behaviour of cold-formed singly symmetric columns". In: *Thin-walled structures* 33.2, pp. 83–102.

Yun, Xiang and Leroy Gardner (2017). "Stress-strain curves for hot-rolled steels". In: *Journal of Constructional Steel Research* 133, pp. 36–46.